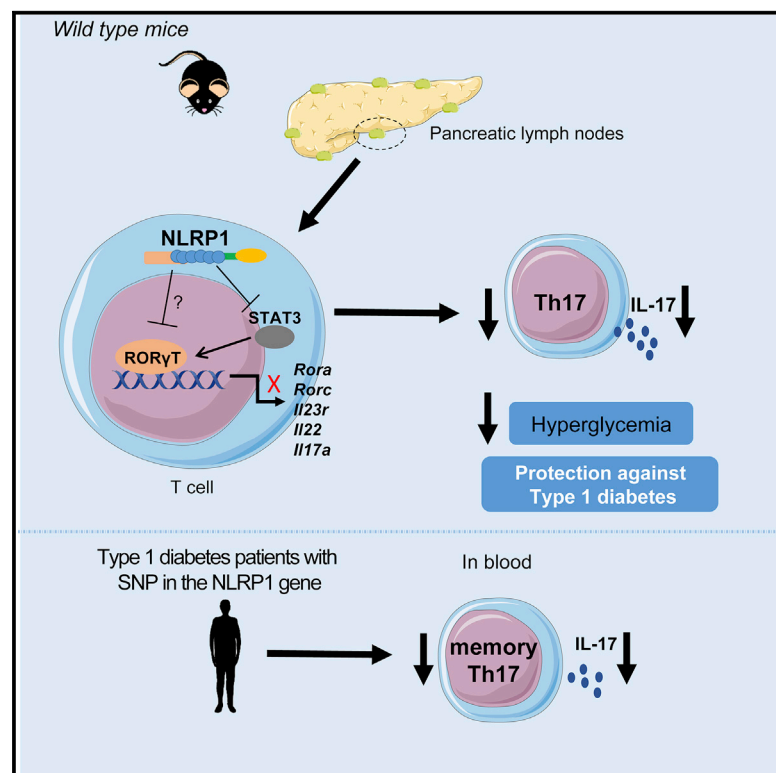


# NLRP1 acts as a negative regulator of Th17 cell programming in mice and humans with autoimmune diabetes

## Graphical abstract



## Authors

Frederico R.C. Costa, Jefferson A. Leite, Diane M. Rassi, ..., Rita C. Tostes, João S. Silva, Daniela Carlos

## Correspondence

danicar@usp.br

## In brief

Costa et al. demonstrate that NLRP1 is important for the differentiation of Th17 cells in both mice and humans with type 1 diabetes. Mechanistically, *Nlrp1b* expressed by T cells suppresses ROR $\gamma$ t in a STAT3-dependent pathway, thus, negatively regulating the differentiation of Th17 cells.

## Highlights

- NLRP1 has a role in both mouse and human autoimmune diabetes
- NLRP1 expressed by T cells downregulates the differentiation of Th17 cells
- NLRP1, in a STAT3-dependent pathway, suppresses Th17-signature genes, such as ROR $\gamma$ t
- IL-17 levels are decreased in T1D patients carrying a SNP (rs12150220) in the NLRP1 gene



## Article

# NLRP1 acts as a negative regulator of Th17 cell programming in mice and humans with autoimmune diabetes

Frederico R.C. Costa,<sup>1</sup> Jefferson A. Leite,<sup>1</sup> Diane M. Rassi,<sup>2</sup> Josiane F. da Silva,<sup>2</sup> Jefferson Elias-Oliveira,<sup>1</sup> Jhefferson B. Guimarães,<sup>1</sup> Maria C. Foss-Freitas,<sup>3,4</sup> Niels O.S. Câmara,<sup>5,6</sup> Alessandra Pontillo,<sup>6</sup> Rita C. Tostes,<sup>2</sup> João S. Silva,<sup>1,7</sup> and Daniela Carlos<sup>1,8,\*</sup>

<sup>1</sup>Department of Biochemistry and Immunology, Ribeirão Preto Medical School, University of São Paulo, Ribeirão Preto, SP, Brazil

<sup>2</sup>Department of Pharmacology, Ribeirão Preto Medical School, University of São Paulo, Ribeirão Preto, SP, Brazil

<sup>3</sup>Department of Clinical Medicine, Internal Medicine Division, Ribeirão Preto Medical School, University of São Paulo, Ribeirão Preto, SP, Brazil

<sup>4</sup>Division of Metabolism, Endocrinology & Diabetes, Department of Internal Medicine, and Caswell Diabetes Institute University of Michigan, Ann Arbor, MI, USA

<sup>5</sup>Department of Immunology, Federal University of São Paulo (UNIFESP), São Paulo, SP, Brazil

<sup>6</sup>Department of Immunology, Institute of Biomedical Sciences (ICB), University of São Paulo, São Paulo, SP, Brazil

<sup>7</sup>Fiocruz- Bi-Institutional Translational Medicine Platform, Ribeirão Preto, SP, Brazil

<sup>8</sup>Lead contact

\*Correspondence: [danicar@usp.br](mailto:danicar@usp.br)

<https://doi.org/10.1016/j.celrep.2021.109176>

## SUMMARY

Type 1 diabetes (T1D) is an autoimmune disease characterized by the destruction of pancreatic  $\beta$  cells. We show here that the protein NOD-like receptor family pyrin domain containing 1 (NLRP1) has a key role in the pathogenesis of mouse and human T1D. More specifically, downregulation of NLRP1 expression occurs during T helper 17 (Th17) differentiation, alongside greater expression of several molecules related to Th17 cell differentiation in a signal transducers and activators of transcription 3 (STAT3)-dependent pathway. These changes lead to a consequent increase in interleukin 17 (IL-17) production within the pancreas and higher incidence of diabetes in streptozotocin (STZ)-injected mice. Finally, in patients with T1D and a SNP (rs12150220) in *NLRP1*, there is a robust decrease in IL-17 levels in serum and in memory Th17 cells from peripheral blood mononuclear cells. Our results demonstrate that NLRP1 acts as a negative regulator of the Th17 cell polarization program, making it an interesting target for intervention during the early stages of T1D.

## INTRODUCTION

Type 1 diabetes (T1D) is a T-cell-mediated disease characterized by the autoimmune destruction of insulin-producing pancreatic  $\beta$  cells (Atkinson et al., 2014; Haller et al., 2018). The incidence of the disease has increased during the past 30 years (Patterson et al., 2009), which can only be explained by alterations in the environment or lifestyle (Rewers and Ludvigsson, 2016). In that context, several environmental factors have been proposed as possible triggers for this disease, such as viral infections (Filippi and von Herrath, 2008) and alterations in the composition of the gut microbiota (dysbiosis) (Vaarala, 2008). Thus, a better understanding of the environmental triggers involved in the development of T1D is of extreme importance to delay or even prevent the onset of the disease. Most of our knowledge on the pathophysiology of T1D comes from studies on the adaptive immune response, demonstrating a pathogenic role for both T helper 1 (Th1) (Arif et al., 2011) and Th17 (Honkanen et al., 2010) cells. Although studies on the role of the innate immune response in the development of T1D

are scarce (Herold et al., 2013), macrophages have been identified in the pancreas of patients with T1D (Uno et al., 2007), and dendritic cells (DCs) were shown to capture antigens released by apoptotic  $\beta$  cells and present them to antigen-specific T cells in the pancreatic lymph nodes (PLNs) (Marleau et al., 2008). Surprisingly, despite several studies demonstrating the presence of cells from the innate immune response in the pathogenesis of T1D, the mechanisms by which pattern-recognition receptors (PRRs) are activated in these cells and how they initiate the autoimmune destruction of the insulin-producing pancreatic  $\beta$  cells remain poorly understood. Our group and others have shown that the lack of the NOD-like receptor family pyrin domain containing 3 (NLRP3), a member of the NOD-like receptor (NLR) family, protects both nonobese diabetic (NOD) and streptozotocin (STZ)-injected C57BL/6 mice from developing diabetes (Carlos et al., 2017; Hu et al., 2015). Toll-like receptor 2 (TLR2) also has a pathogenic role in the disease, through the production of proinflammatory cytokines, such as interleukin-1 $\beta$  (IL-1 $\beta$ ), IL-12p70, and nitric oxide (NO) (Kim et al., 2007). Therefore, it is critical to better understand the



role of PRRs in the context of T1D to pursue new therapeutic strategies that may prevent the onset of the disease.

The NOD-like receptor family pyrin domain containing 1 (NLRP1) is a member of the NLR family that assembles a complex called inflammasome, which ultimately leads to the cleavage of pro-IL-1 $\beta$  and pro-IL-18 into their mature forms through the oligomerization of apoptosis-associated speck-like protein (ASC) and consequent activation of caspase-1 in myeloid cells (Shimada et al., 2012). NLRP1 is expressed by several cell types, which are mostly hematopoietic. Nonetheless, expression has also been found within glandular epithelial structures, including the lining of the small intestine, stomach, and colon (Tye et al., 2018). Human *NLRP1* possesses three paralog genes in mice (*Nlrp1a*, *Nlrp1b*, and *Nlrp1c*), which, in turn, are extremely polymorphic between distinct isogenic strains (Boyden and Dietrich, 2006). These variations between mouse strains in the *Nlrp1b* locus seem to be responsible for the different responses observed after stimulation with the lethal toxin (LT) from *Bacillus anthracis*, considering that macrophages from susceptible, but not resistant, mouse strains are capable of activating caspase-1 after exposure to LT (Boyden and Dietrich, 2006). *Nlrp1a*, on the other hand, has been shown to induce pyroptosis in hematopoietic progenitor cells in a caspase-1-dependent pathway, leading to a state of immunosuppression in mice with an activating mutation in *Nlrp1a* (Masters et al., 2012). In addition, *Nlrp1a* induces dysbiosis through the production of interferon- $\gamma$  (IFN- $\gamma$ ) and IL-18, aggravating dextran sulfate sodium (DSS)-induced experimental mouse colitis (Tye et al., 2018). Collectively, these data suggest distinct roles for NLRP1 depending on the pathophysiological context, thus, prompting more studies to better characterize its role in distinct pathologies. In the context of T1D, there are only a few reports in the literature that relate the presence of polymorphisms in *NLRP1*, such as rs12150220, with the development of human T1D (Magitta et al., 2009; Tang et al., 2013) or with protection from diabetic nephropathy in T1D patients (Soares et al., 2017). However, the importance of this receptor, as well as the cytokines produced by its activation in the induction of an inflammatory response and further polarization of the immune response toward a proinflammatory milieu during T1D development, has not been investigated. Thus, we aimed to determine the role of NLRP1 both in an experimental mouse model and in humans with T1D. Our data provide evidence that NLRP1 acts as a negative regulator of the Th17 cell programming in murine models of T1D through the activation of *Nlrp1b* in lymphoid cells and also in humans with T1D. In addition, NLRP1, through the activation of *Nlrp1a*, is an important receptor in maintaining the integrity of the gut epithelial barrier, thus, dampening the translocation of bacteria from the gut during STZ-induced T1D and, consequently, delaying the onset of the disease.

## RESULTS

### NLRP1 has a protective role in STZ-induced T1D

To investigate the possible role of NLRP1 in T1D, wild-type (WT) mice, or mice that are deficient for all three paralog genes (*Nlrp1a,b,c*<sup>−/−</sup>, hereafter referred to as NLRP1<sup>−/−</sup> mice) were injected with five doses of STZ and had their blood glucose levels

analyzed at days 10 and 15 after the first dose (Figure 1A). Interestingly, we observed that STZ-injected NLRP1<sup>−/−</sup> presented higher glycemia levels at days 10 and 15 compared with STZ-injected WT mice (Figures 1B and 1C, respectively). Although diabetes (blood glucose levels greater than 200 mg/dL) initiated already at day 10 in NLRP1<sup>−/−</sup> mice, WT mice exhibited an incidence peak only at day 15, thus, suggesting a protective role for this receptor in the development of STZ-induced T1D. In addition, histopathological analysis showed an increase in the inflammatory infiltrate (insulitis) in the pancreatic islets of NLRP1-deficient mice, compared with WT mice, already at day 10 after STZ injections. Of note, 15 days after the injections, in which most of both WT and NLRP1<sup>−/−</sup> mice had become diabetic, such differences were lost, and both groups displayed robust insulitis within the pancreas (Figures 2D and 2E).

### NLRP1 restrains the differentiation of IL-17-producing T cells in the PLNs during STZ-induced T1D onset

To determine whether NLRP1 is involved in the induction of pathogenic T cells that contribute to T1D development, the frequency and absolute numbers of Th1, Tc1, Th17, and Tc17 were analyzed in the PLNs of WT and NLRP1<sup>−/−</sup> mice, injected with vehicle or STZ, at days 10 and 15 after the first dose. Ten days after the first STZ injection, there were no differences in Th1 or Tc1 cells between groups (Figure 2A). However, an increase in both frequency and absolute numbers of Th17 and Tc17 cells were observed in the PLNs of NLRP1<sup>−/−</sup> mice injected with STZ, when compared with their WT counterparts (Figure 2B), thus, indicating a possible role for IL-17-producing T cells in the increased susceptibility to STZ-induced T1D by NLRP1<sup>−/−</sup> mice. Interestingly, a higher IL-17 percentage was already observed in NLRP1<sup>−/−</sup> injected with vehicle solution, indicating that, in the absence of such receptor, there is already a higher proportion of Th17 cells in the PLNs at baseline (Figure 2B). Additionally, an increased production of IL-6, but not IL-12, by DCs within the PLNs was observed (Figure 2C), which corroborates the increased Th17 population found in the PLNs.

Interestingly, 15 days after the STZ injections, there was an increase in Th1, Tc1, Th17, and Tc17 cells in the PLNs of STZ-injected WT mice (Figures S1A and S1B), which reconciles with the incidence peak of the disease observed in those mice (Figure 1C). Surprisingly, in STZ-injected NLRP1<sup>−/−</sup> mice, there was also the induction of Th1 and Tc1 cells, and the initial increase in IL-17-producing T cells observed at day 10 (Figure 2B) was lost 15 days after the STZ injections (Figures S1A and S1B). These data suggest that NLRP1 is important in the regulation of Th17 and Tc17 cells during the initial stages of STZ-induced T1D.

Considering the intimate relationship between Th17 cells and regulatory T (Treg) cells mediated by the shared common signaling pathway of transforming growth factor  $\beta$  (TGF- $\beta$ ) (Lee, 2018), we also analyzed the presence of Treg cells in NLRP1<sup>−/−</sup> mice during STZ-induced T1D to investigate whether an imbalance in the Treg/Th17 axis was also contributing to the increased susceptibility of NLRP1-deficient mice to STZ-induced T1D. As shown in Figure 2D, there was a downregulation in the frequency of Treg cells in STZ-injected NLRP1<sup>−/−</sup> mice, yet no differences were found in terms of absolute numbers (Figure 2D). However, despite the shift in the Treg/Th17 axis toward

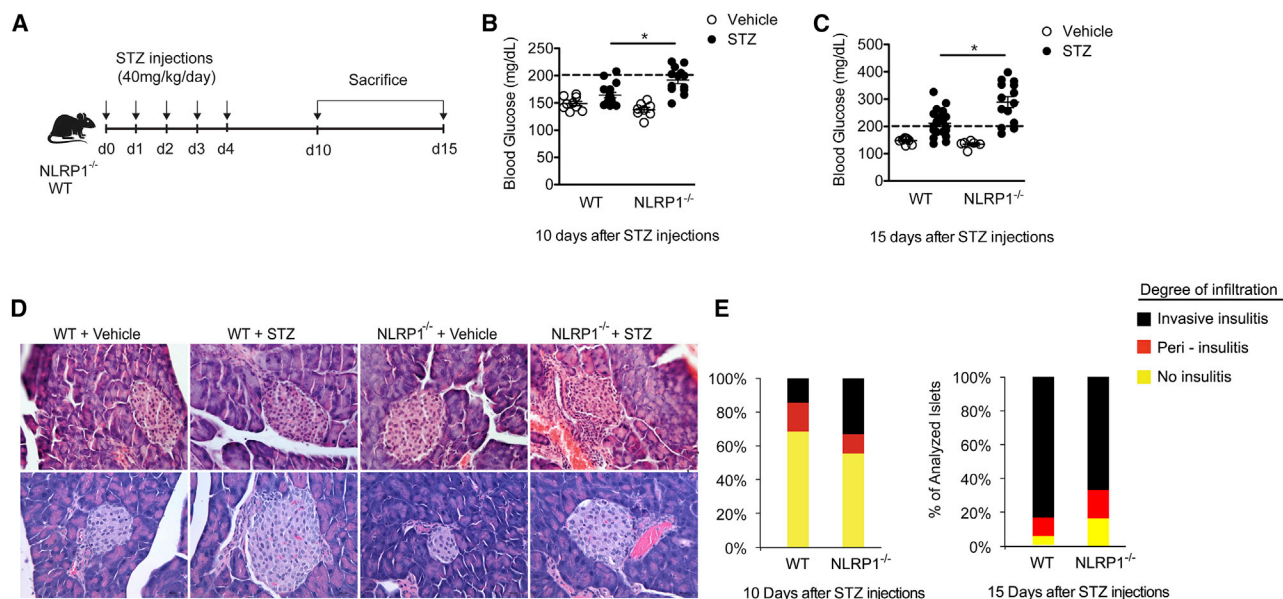


**Figure 1. NLRP1 has a protective role in STZ-induced T1D**

(A) WT and NLRP1<sup>-/-</sup> mice were injected with five doses of STZ (40 mg/kg/day) or vehicle solution (control).

(B and C) Blood glucose levels were determined at days 10 (B) and 15 (C) after the STZ injections.

(D and E) Their pancreata were collected and stained with hematoxylin and eosin (H&E) for histopathological analysis 10 (top panel) or 15 (bottom panel) days after the STZ injections and also for the analysis of insulinitis.

The results are a compilation of three independent experiments and are expressed as the means  $\pm$  SEM. \* $p \leq 0.05$  was considered statistically significant.

a proinflammatory phenotype, we believe that Treg cells alone are not involved in the increased susceptibility of NLRP1<sup>-/-</sup> mice to STZ-induced T1D. Finally, to further confirm the importance of the increased numbers of Th17 cells in the PLNs to the T1D outcome, WT and NLRP1<sup>-/-</sup> mice were injected with a neutralizing anti-IL17A antibody in the beginning of the STZ regime (Figure 2E). Surprisingly, the blockade of IL-17 was able not only to rescue mice from developing hyperglycemia in both WT and NLRP1<sup>-/-</sup> mice (blood glucose levels greater than 200 mg/dL) but also to abrogate the difference in blood glucose levels between WT and NLRP1<sup>-/-</sup> reported in Figure 1C. Overall, these data indicate that the increased susceptibility of NLRP1-deficient mice to STZ-induced T1D is Th17-cell dependent.

Next, levels of proinflammatory cytokines in the pancreas, which is the target organ of the disease, were determined in those mice. Both IL-17 and IFN- $\gamma$  were intimately related with the destruction of the insulin-producing  $\beta$  cells, with a consequent state of hyperglycemia. As demonstrated in Figure 3A, there is a strong positive correlation between IFN- $\gamma$  and IL-17 levels in the pancreas and the blood glucose levels of WT injected with STZ. As expected, no differences were found in IFN- $\gamma$  levels in the pancreas at days 10 and 15 of either WT or NLRP1<sup>-/-</sup> mice injected with STZ (Figures 3B and 3C, respectively). Surprisingly, there were no differences in IL-17 levels at day 10 (Figure 3B). However, when STZ-injected NLRP1<sup>-/-</sup> mice at 10 days were divided into mice that had already become diabetic (red circles) and non-diabetic mice (black circles), a statistical difference in IL-17 levels between diabetic NLRP1<sup>-/-</sup> mice and STZ-injected WT mice was observed, thus, corroborating

a pathogenic role for IL-17 in the destruction of the pancreatic  $\beta$  cells (Figure 3B). Of note, no statistical differences were observed in IFN- $\gamma$  levels when the same division (diabetic versus non-diabetic STZ-injected NLRP1<sup>-/-</sup> mice) was performed (data not shown). Even though there was an increase in IL-17 levels in the pancreatic tissue at day 10 (levels ranged from  $\sim 3$  to  $\sim 6$  ng/g in both groups), no differences were found between NLRP1<sup>-/-</sup> and WT mice at 15 days after the STZ injections, corroborating the data from the PLNs (Figure 3C). Collectively, these data suggest a protective role for NLRP1 in STZ-induced T1D through the negative regulation of IL-17 expression during the early stages of the disease.

Considering that *Nlrp1a-c* genes are highly polymorphic between distinct isogenic strains (Boyden and Dietrich, 2006), their expression in NOD mice was also analyzed. Interestingly, we observed an increase in both *Nlrp1a* and *Nlrp1b* levels in the pancreas of NOD mice during later stages of the disease because a statistical difference was only observed at the 20th week (Figure 3D). Surprisingly, the *il17* gene was also expressed, however, at earlier stages of the disease (10th week). At the peak of *Nlrp1a* and *Nlrp1b* gene expression, IL-17 levels (both RNA and protein) returned to baseline, which suggest a similar mechanism of NLRP1 downregulating IL-17 expression in both STZ-induced T1D and NOD mice.

### The gut microbiota contributes to increased T1D susceptibility, but not to increased IL-17 levels, in NLRP1-deficient mice

Our group has recently shown that gut microbiota translocation to the PLNs is of extreme importance to the development of



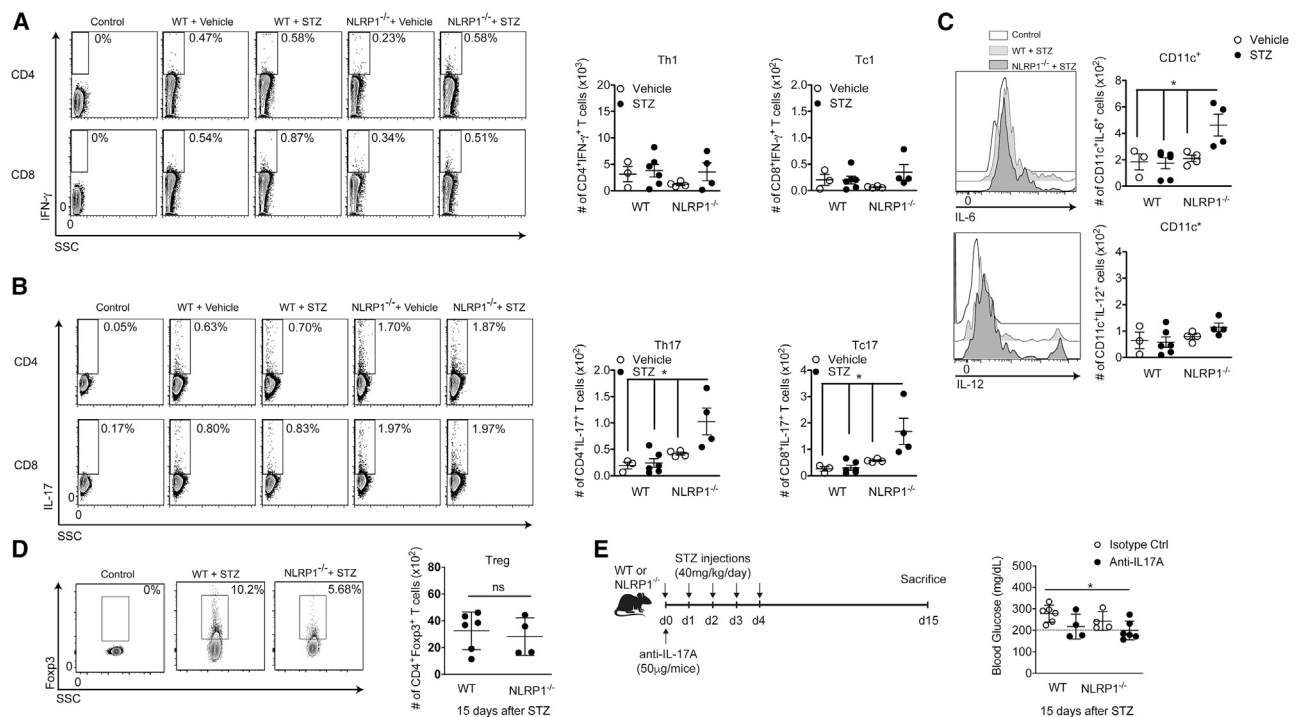


**Figure 2. NLRP1 inhibits Th17 cells during the early stages of STZ-induced T1D**

(A–C) WT and NLRP1<sup>-/-</sup> mice were injected with five doses of STZ (40 mg/kg/day) or vehicle solution (control). These animals were then sacrificed, and the pancreatic lymph nodes (PLNs) were collected at day 10 for the analysis of the frequency and absolute numbers of Th1 (CD4<sup>+</sup>IFN- $\gamma$ <sup>+</sup>), Tc1 (CD8<sup>+</sup>IFN- $\gamma$ <sup>+</sup>), Th17 (CD4<sup>+</sup>IL-17<sup>+</sup>), Tc17 (CD8<sup>+</sup>IL-17<sup>+</sup>) (A and B), and IL-6- and IL-12-producing dendritic cells (C) by flow cytometry.

(D) Alternatively, STZ-injected WT and NLRP1<sup>-/-</sup> mice were sacrificed 15 days after the STZ injections, and the PLNs were collected for the analysis of the frequency and absolute numbers of Treg (CD4<sup>+</sup>Foxp3<sup>+</sup>) cells.

(E) In another set of experiments, WT and NLRP1<sup>-/-</sup> mice were injected with five doses of STZ (40 mg/kg/day). On the first day of the STZ injections, mice were also injected with a neutralizing anti-IL-17A antibody or an isotype control. Blood glucose levels were determined 15 days after the STZ injections.

The results are representative of at least two independent experiments and are expressed as the means  $\pm$  SEM. \* $p \leq 0.05$  was considered statistically significant.

STZ-induced T1D (Costa et al., 2016). Thus, we hypothesized that the increase in Th17 cells, and consequent increment in the susceptibility of NLRP1<sup>-/-</sup> mice to develop STZ-induced T1D, could be attributed to a higher translocation of bacteria from the gut to the PLNs. Thus, the presence of bacteria in the PLNs of WT and NLRP1<sup>-/-</sup> mice treated with vehicle or STZ was determined. Interestingly, both naive and STZ-injected NLRP1<sup>-/-</sup> mice presented higher levels of gut bacteria translocation to the PLNs at 10 and 15 days after the STZ injections when compared with that of WT mice (injected with vehicle or STZ), thus, suggesting a possible role for NLRP1 in the integrity of the gut-epithelial barrier (Figure S2A). The expression of *Nlrp1a* and *Nlrp1b* genes in the ileum of naive and STZ-injected WT mice was also analyzed. An increase in *Nlrp1a*, but not *Nlrp1b*, expression was observed during the development of the disease (Figure S2B), which corroborates the work of Tye et al. (2018) showing a more prominent role for *Nlrp1a* within the intestinal tissue.

To further confirm that the gut microbiota is involved in the increased susceptibility of NLRP1<sup>-/-</sup> mice to STZ-induced T1D, mice were treated with a cocktail of antibiotics (Abx) for 3 weeks to reduce the number of bacteria present in the gastrointestinal tract. Then, they were injected with five doses of STZ (Figure S2C). Alternatively, another group of NLRP1<sup>-/-</sup> mice

was submitted to the Abx treatment, but, after the Abx treatment, they were also transplanted with feces from WT mice (NLRP1<sup>-/-</sup>[WT] group). Ten days after the fecal transplantation, which is the necessary time period for the bacteria to colonize the intestinal tract, mice were injected with STZ (Figure S2C). Surprisingly, the treatment with the Abx cocktail inhibited the development of STZ-induced T1D in NLRP1-deficient mice, making them fully resistant to the disease (Figure S2D). In addition, even harboring a different gut microbiota composition (NLRP1<sup>-/-</sup>[WT] group), these fecal-transplanted NLRP1<sup>-/-</sup> mice also developed the disease, with greater incidence, when compared with that of WT mice. Collectively, these data suggest that augmented bacterial translocation to the PLNs of NLRP1<sup>-/-</sup> mice is involved in the increased susceptibility to STZ-induced T1D.

Lastly, we analyzed whether the gut microbiota is intimately related to the increased Th17 levels presented by NLRP1<sup>-/-</sup> mice injected with STZ. Interestingly, NLRP1<sup>-/-</sup> mice submitted to the Abx cocktail regimen and injected with STZ presented similar levels of Th17 cells when compared with STZ-injected NLRP1<sup>-/-</sup> mice that were not treated with Abx (Figure S2E). These data indicate that the gut microbiota is not responsible for the increased levels of Th17 cells displayed by STZ-injected NLRP1<sup>-/-</sup> mice.

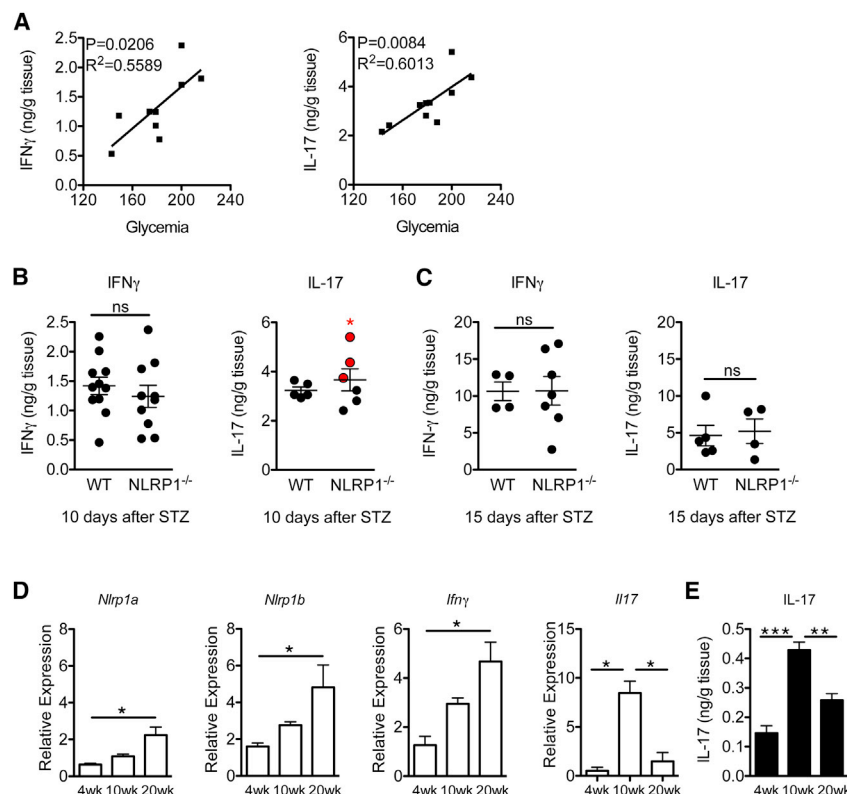


**Figure 3. NLRP1 is also associated with diabetes development in NOD mice**

(A) WT mice were injected with five doses of STZ (40 mg/kg/day) or vehicle solution (control). Blood glucose levels were analyzed, and pancreata collected at days 10 and 15 for the analysis of cytokine production by ELISA. Glycemia from both WT and NLRP1 $^{-/-}$  was correlated with the production of IFN- $\gamma$  and IL-17.

(B and C) Cytokine production at days 10 (B) and 15 (C) after STZ injections are shown.

(D and E) Alternatively, NOD mice were sacrificed at 4, 10, or 20 weeks of age, and the pancreata was collected for the analysis of *Nlrp1a*, *Nlrp1b*, *Ifn $\gamma$* , and *Il17* mRNA expression by RT-PCR (D) or IL-17 protein expression by ELISA (E).

The results are representative of at least two independent experiments and are expressed as the means  $\pm$  SEM.  $*p \leq 0.05$ ,  $**p \leq 0.005$ ,  $***p \leq 0.001$ .

### Activation of the inflammasome machinery is not involved in the increased susceptibility of NLRP1 $^{-/-}$ mice to STZ-induced T1D

Innate immune receptors are also expressed by T cells, and those receptors have an important role in the differentiation of naive T cells toward different Th subtypes (Arbore et al., 2016; Bruchard et al., 2015; Chen et al., 2009). Thus, we hypothesized that NLRP1 is expressed by T cells and inhibits their differentiation to Th17 cells, which could explain their increase in the PLNs in the absence of the receptor. Thus, the expression of *Nlrp1a* and *Nlrp1b* in lymphoid (CD3 $^{+}$ ), myeloid (CD11b $^{+}$ ), and other cellular subtype (CD3 $^{-}$ CD11b $^{-}$ ) cells in mice that were injected or not with STZ, was analyzed (Figures S3A and S3B). Surprisingly, in contrast to what was observed in the ileum, in which *Nlrp1a* is expressed during diabetes development (Figure 5B), the levels of *Nlrp1a* expression remained unaltered (Figure S3A). Interestingly, *Nlrp1b* was highly expressed, already by day 7 in lymphoid cells, and its expression was maintained throughout the analyzed period (Figure S3B). *Nlrp1b* was also expressed in myeloid cells at day 10, indicating possible activation of the inflammasome through the NLRP1 receptor.

Next, to further validate or exclude the hypothesis that the inflammasome machinery is associated with increased Th17 cells in the absence of NLRP1, several molecules associated with the inflammasome were determined. For that, WT and NLRP1 $^{-/-}$  mice, injected with vehicle or STZ, were sacrificed 10 or 15 days after vehicle/STZ administration, and their pancreata were collected to analyze cytokine production. In the absence of NLRP1, there was a decrease in the production of cytokines

linked to the inflammasome platform, such as IL-1 $\beta$  and IL-18 (Figure S3C). Such a decrease occurred at day 10, but not at day 15 (Figure S3D), which reconciles with the expression of *Nlrp1b* in myeloid cells (Figure S3B). The production of IL-1 $\alpha$ , a cytokine that does not require cleavage by caspase-1 and is found in its mature form, was also determined. As expected, no differences were found in IL-1 $\alpha$  levels 10 or 15 days after STZ injections (Figures S3C and S3D). These data suggest that, even in the absence of proinflammatory cytokines, such as IL-1 $\beta$  and IL-18, NLRP1 $^{-/-}$  mice are still capable of producing a potent Th17 cell immune response, which, in turn, contributes to the early manifestation of STZ-induced T1D in these mice.

Then, to exclude the possibility that the NLRP1 inflammasome is related to the increased susceptibility of NLRP1 $^{-/-}$  mice to STZ-induced T1D, STZ was injected in mice that lack crucial molecules for the assembly of the inflammasome complex, such as caspase-1, caspase-11, ASC, and IL-1R (Figure S3E). Corroborating our hypothesis, none of those animals presented the same phenotype as NLRP1 $^{-/-}$  mice. In fact, mice lacking ASC and IL-1R were actually resistant to STZ-induced T1D.

Collectively, these data indicate that the activation of the inflammasome machinery by the NLRP1 receptor does not protect mice from the development of STZ-induced T1D.

### Inhibition of NLRP1 in lymphocytes is essential for the induction of Th17 cells *in vitro* and *in vivo*

Considering that a robust expression of *Nlrp1b* in lymphoid cells was observed (Figure 3B), our next step was to investigate whether there is a correlation between the expression of *Nlrp1b* and the production of IL-17. Therefore, naive CD4 $^{+}$  T cells were isolated from the lymph nodes and spleen of WT mice and were differentiated toward a Th17 phenotype with polarizing cytokines. Surprisingly, a robust decrease in *Nlrp1b* gene expression and NLRP1 protein levels occurred during the differentiation of Th17 cells, thus indicating that NLRP1 inhibition is necessary

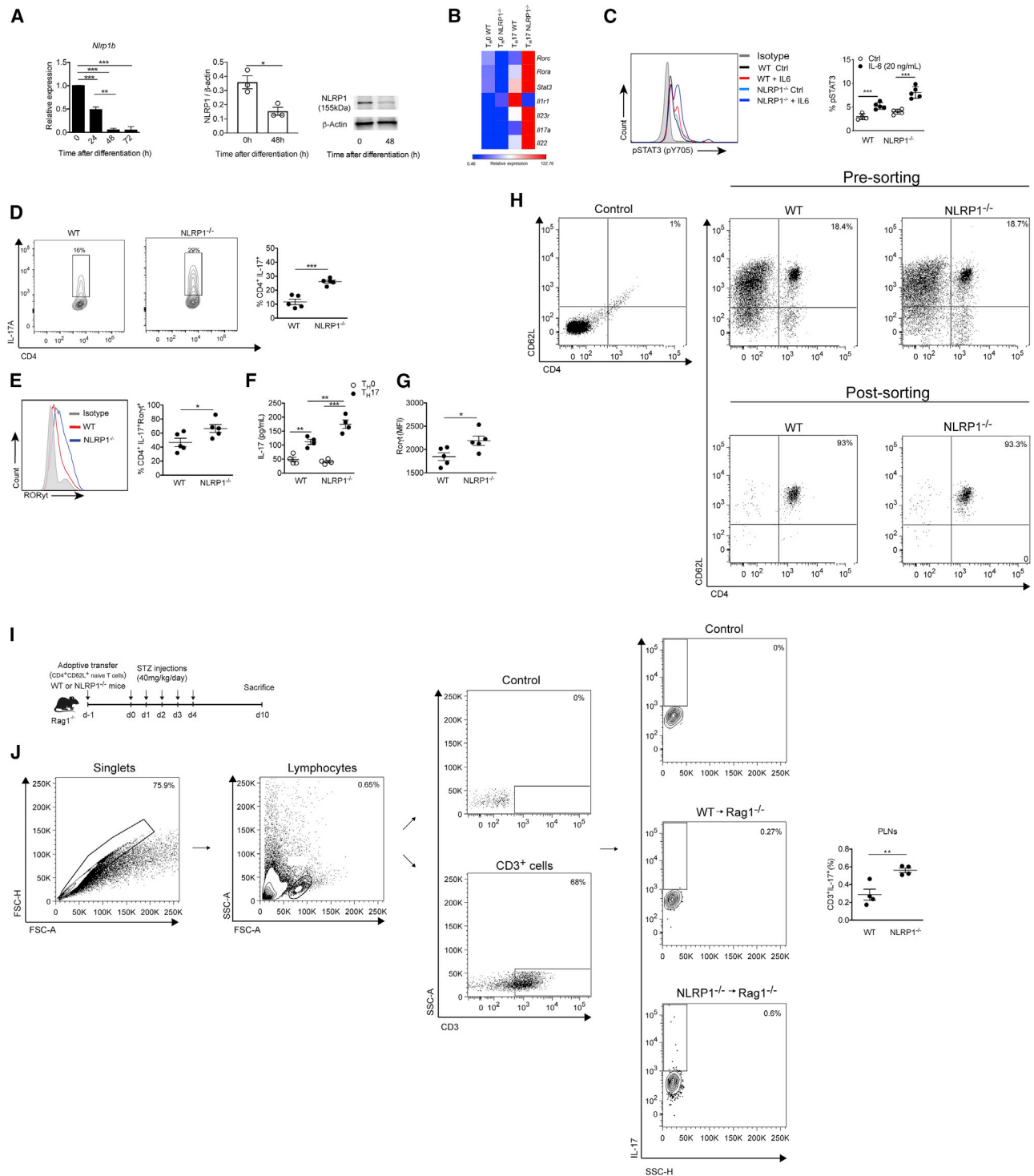


**Figure 4. NLRP1 inhibition is essential for the induction of a Th17 cell immune response**

(A and B) Naive CD4<sup>+</sup> T cells isolated from the spleen and lymph nodes were activated with anti-CD3 and anti-CD28 and were further stimulated *in vitro* with TGF-β, IL-6, IL-23, and IL-1β for the differentiation into Th17 cells. Subsequently, the gene relative expression of *Nlrp1b* (A), *Rorc*, *Rora*, *Stat3*, *Il1r1*, *Il23r*, *Il17a*, and *Il22* (B) was analyzed by RT-PCR and protein levels of NLRP1 were assessed by western blot (B).

(C) In another set of experiments, naive CD4<sup>+</sup> T cells from WT and NLRP1<sup>-/-</sup> mice were isolated from the spleen and lymph nodes and were then stimulated with IL-6 for 30 min. Then, cells were collected and analyzed for phosphorylation levels of STAT3 (pY705) by flow cytometry.

(legend continued on next page)

for the acquisition of a Th17 phenotype (Figure 4A). Next, naive CD4<sup>+</sup> T cells were isolated from WT or NLRP1<sup>-/-</sup> mice and were differentiated into Th17 cells *in vitro* (Figure 4B). They were then analyzed for expression of molecules associated with the Th17 phenotype. Notably, in the absence of NLRP1 during the differentiation of Th17 cells, there was a robust increase in *Rorc*, *Rora*, *Stat3*, *Il23r*, *Il17a*, and *Il22* gene expression (Figure 4B), confirming that NLRP1 represses the expression of several molecules that are crucial for the acquisition of a Th17 phenotype.

Considering that signal transducers and activators of transcription 3 (STAT3) was increased in NLRP1<sup>-/-</sup> cells during the differentiation of Th17 cells and that such a molecule has a pivotal role in IL-6-mediated Th17 cell differentiation (Yang et al., 2007), we also analyzed whether NLRP1 could interfere with such interaction. Thus, CD4<sup>+</sup> T cells from WT or NLRP1<sup>-/-</sup> mice were stimulated with IL-6 and analyzed for pSTAT3 (Y705). Surprisingly, in the absence of NLRP1, there was a robust increase in the phosphorylation of STAT3 when compared with that of WT cells, thus indicating that NLRP1 negatively regulates Th17 cell differentiation through STAT3 phosphorylation (Figure 4C). Finally, protein levels of IL-17 and ROR $\gamma$ t were analyzed by either ELISA or flow cytometry. As expected, there was a robust increase in the frequency of CD4<sup>+</sup>IL-17<sup>+</sup> (Figure 4D) and CD4<sup>+</sup>IL-17<sup>+</sup>ROR $\gamma$ t<sup>+</sup> (Figure 4E) cells, as well as in IL-17 protein levels in the supernatant of NLRP1<sup>-/-</sup> cells compared with that of WT cells (Figure 4F). Increased expression of ROR $\gamma$ t was also observed (Figure 4G), suggesting that increased IL-17 production in the absence of NLRP1 may be attributed to a positive regulation of the Th17's master regulator, ROR $\gamma$ t. To further assess the importance of NLRP1 in inhibiting the differentiation of Th17 cells, *in vivo* experiments were also performed. Isolated CD4<sup>+</sup> T cells from WT or NLRP1<sup>-/-</sup> mice were adoptively transferred to Rag1<sup>-/-</sup> mice. Subsequently, those mice were injected with five doses of STZ and were sacrificed 10 days later to analyze the presence of Th17 cells in the PLNs (Figures 4H and 4I). An increased frequency of Th17 cells was observed in Rag1<sup>-/-</sup> mice transferred with NLRP1<sup>-/-</sup> cells when compared with that of Rag1<sup>-/-</sup> mice harboring WT cells (Figure 4J), which also corroborates our *in vitro* findings. Overall, these data indicate that NLRP1 acts as a negative regulator of Th17 cell differentiation by controlling the STAT3-ROR $\gamma$ t axis.

### NLRP1 is also a negative regulator of Th17 cells in humans with T1D

Finally, in an attempt to translate these findings to patients with T1D, we questioned whether the human receptor functions similarly to mouse *Nlrp1b*. For that, the single-nucleotide polymorphism (SNP) rs12150220 A>T was selected to perform a geno-

type-guided assay with peripheral blood mononuclear cells (PBMCs) isolated from patients with T1D. This variant corresponds to a leucine-to-histidine amino acid change at position 155 (Leu155His) of the NLRP1 receptor (Levandowski et al., 2013) and has been extensively associated with several autoimmune diseases, including T1D (Magitta et al., 2009; Soares et al., 2017; Tang et al., 2013).

The SNP was genotyped in a cohort of patients with T1D (n = 79). The genotype distribution of rs12150220 A>T variant, as well as the main characteristics of the T1D cohort, is reported in Table S1. NLRP1 expression in PBMCs, lymphocytes subpopulations, and lymphocyte cytokine production were determined and compared between patients with T1D carrying the SNP (rs12150220) or not (WT), according to a recessive model of inheritance (T/T versus A/A + A/T).

As observed in Figure 5A, there was no difference in NLRP1 expression between carriers of polymorphic homozygote T/T and the WT group, which reconciles with the work from Levandowski et al. (2013), showing that such SNP in NLRP1 is not associated with differences in mRNA expression. The frequency of CD3<sup>+</sup> T cells and CD4<sup>+</sup> T cells was then determined, and again, no statistical differences were found between the rs12150220 and WT groups (Figures 5B and 5C, respectively). Lastly, the frequency of Th1 and Th17 cells was analyzed. No differences were found in Th1 cells between the two groups (Figure 5D). A tendency, without statistical significance, toward a decrease in Th17 cell population was found in patients harboring the mutation (Figure 5E).

Considering that most of our cohort had displayed the disease for more than 15 years (Table S1), we hypothesized that most of the effector autoreactive response was found within the memory compartment, as previously reported (Spanier et al., 2017). Thus, we determined the frequency of IFN- $\gamma$ - and IL-17-producing memory (CD45RO<sup>+</sup>CD45RA<sup>-</sup>) T cells in PBMCs from WT and rs12150220 T1D patients. Surprisingly, a robust decrease in memory Th17 cells was found in patients carrying the rs12150220 variant in homozygosis, whereas no differences were found in Th1 cells (Figures 5F and 5G, respectively). In addition, the production of IL-17 and IFN- $\gamma$  in the serum of those patients was analyzed. Corroborating the cytometry data, a robust decline in the production of IL-17, but not in IFN- $\gamma$  production, was observed in the rs12150220 group.

The present study demonstrates that the polymorphism rs12150220, in addition to its previously described effect on IL-1 $\beta$  production (Levandowski et al., 2013), is associated with lower levels of Th17 cells in patients with T1D. Considering that this NLRP1 variant has been associated with increased inflammasome activation (Levandowski et al., 2013), these findings support the hypothesis of a negative effect of NLRP1 inflammasome activation on Th17 lymphocytes.

(D, E, and G) Alternatively, isolated CD4<sup>+</sup>T cells from WT and NLRP1<sup>-/-</sup> mice were polarized *in vitro* into Th17 cells and were analyzed for the frequency of Th17 cells, as well as the mean fluorescence index (MFI) of ROR $\gamma$ t.

(F) Protein levels of IL-17 in the supernatant were measured by ELISA.

(H) Alternatively, isolated, naive T cells from WT and NLRP1<sup>-/-</sup> were adoptively transferred to Rag1<sup>-/-</sup> mice.

(I and J) These animals were then injected with five doses of STZ, sacrificed at day 10, and the PLNs were used to determine the frequency of Th17 cells by flow cytometry.

The results are representative of at least two independent experiments and are expressed as the means  $\pm$  SEM. \*p  $\leq$  0.05, \*\*p  $\leq$  0.005, \*\*\*p  $\leq$  0.0005.



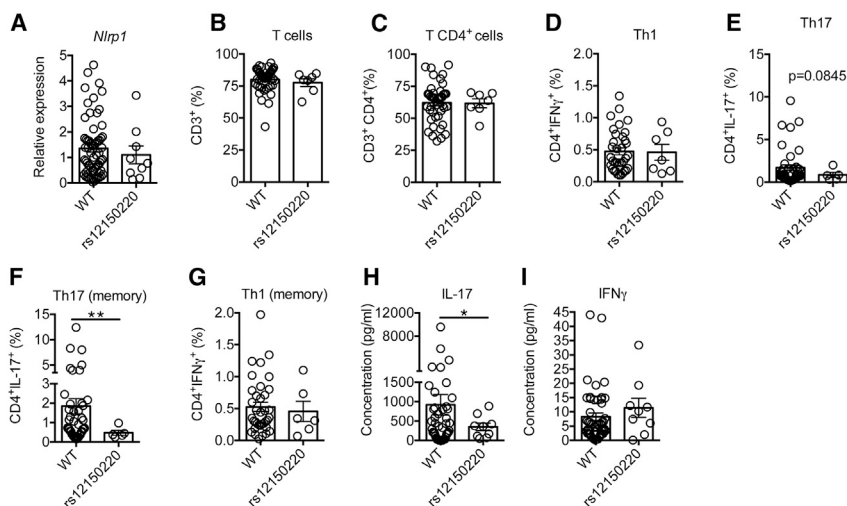


**Figure 5. NLRP1 activation is also linked to decreased Th17 cells in humans with T1D**

(A–G) Blood from patients with T1D harboring, or not harboring, the mutation in NLRP1 rs12150220 was collected for the isolation of PBMCs. mRNA expression of *Nlrp1* by RT-PCR (A), and the frequency of CD3<sup>+</sup> T (B), CD4<sup>+</sup> T (C), Th1 (CD3<sup>+</sup>CD4<sup>+</sup>IFN-γ<sup>+</sup>) (D), Th17 (CD3<sup>+</sup>CD4<sup>+</sup>IL-17<sup>+</sup>) (E), memory Th17 (CD3<sup>+</sup>CD45RO<sup>+</sup>CD45RA<sup>+</sup>CD4<sup>+</sup>IL-17<sup>+</sup>) (F), and memory Th1 (CD3<sup>+</sup>CD45RO<sup>+</sup>CD45RA<sup>+</sup>CD4<sup>+</sup>IFN-γ<sup>+</sup>) (G) cells, by flow cytometry was then determined.

(H and I) Alternatively, sera collected from the patients were used for the analysis of IFN-γ (H) and IL-17 (I) production by ELISA.

The results are expressed as the means ± SEM. \*p ≤ 0.05, \*\*p ≤ 0.005.

## DISCUSSION

The pathogenic role of T cells in T1D is well documented (reviewed by Walker and von Herrath, 2016). However, the role of the innate immune response in the pathogenesis of the disease remains elusive. In this context, NOD mice deficient for TLR2 (Kim et al., 2007), but not the STZ mouse model (Devaraj et al., 2011), are resistant to T1D development. In addition, our research group has recently demonstrated that the innate immune sensors NLRP3 (Carlos et al., 2017) and NOD2 (Costa et al., 2016) have a detrimental role in the development of STZ-induced T1D, which was also confirmed in NOD mice (Hu et al., 2015; Li et al., 2017), even though those receptors signal differently in those two mouse models of diabetes. The present study demonstrates that the innate immune receptor NLRP1 has a protective role in T1D, considering that, in the absence of the receptor, mice injected with STZ become more susceptible to the disease, displaying a more robust inflammatory infiltrate within the pancreatic islets, which is correlated with an increased adaptive immune response or, more specifically, with increased IL-17-producing T lymphocytes in the PLNs and in the pancreatic tissue.

The role of IL-17 in T1D remains controversial. Silencing of IL-17 does not protect NOD mice from the development of the disease (Joseph et al., 2012). On the other hand, a pathogenic role for this cytokine in T1D has been demonstrated. For instance, blockade with a monoclonal antibody anti-IL-17 in the effector phase of the disease (10 weeks of age) prevents the onset of T1D in NOD mice (Emamaullee et al., 2009). In the STZ mouse model, similar findings were reported, thus, corroborating a pathogenic role for IL-17 in T1D (Costa et al., 2016; Yaochite et al., 2013). In humans, increased IL-17 production in the serum of patients with T1D was reported (Ferraro et al., 2011), which also reconciles with murine data. In agreement with both mouse models and humans with T1D, we demonstrate that increased IL-17 in the earlier stages of the disease is intimately related to a higher susceptibility to T1D. Interestingly, within the same group (NLRP1<sup>-/-</sup> mice injected with STZ), animals that displayed hyperglycemia had higher levels of IL-17, whereas those that did not

develop diabetes exhibited normal levels of the cytokine. In addition, a robust positive correlation between increased IL-17-producing T cells (Th17 and Tc17) and inflammatory infiltrates, as well as blood glucose levels, was displayed by NLRP1<sup>-/-</sup> mice.

Our next step was to investigate what was causing the increase in IL-17 in mice lacking NLRP1. Our research group has recently shown that the gut microbiota has a critical role in the development of STZ-induced T1D, through bacteria translocation to the PLNs, which, in turn, activates myeloid cells via NOD2, leading to a proinflammatory immune response (increased Th1 and Th17 cells) (Costa et al., 2016). Thus, we questioned whether the gut microbiota was responsible for the induction of Th17 cells in the absence of the NLRP1 receptor. Surprisingly, mice deficient for NLRP1 exhibited an increased bacterial translocation to the PLNs. The presence of bacteria (aerobic and anaerobic) was observed even in naive NLRP1<sup>-/-</sup> mice, suggesting a possible role of this receptor in the integrity of the intestinal epithelial barrier. In this context, other receptors from the NLR family, such as NLRP6 and NLRP12, are important for both the profile of the gut microbiota and the integrity of the intestinal epithelial barrier (Chen, 2014; Elinav et al., 2011; Wlodarska et al., 2014). In addition, increased NLRP1 in the colon from patients with ulcerative colitis (Williams et al., 2015) and a protective role of NLRP1, possibly through *Nlrp1a*, in dextran sodium sulfate (DSS)-induced colitis (Tye et al., 2018) have been reported. Interestingly, diabetic WT mice (that presented lower bacterial translocation toward the PLNs compared with diabetic NLRP1<sup>-/-</sup> mice) exhibited increased *Nlrp1a*, but not *Nlrp1b*, expression in the ileum, thus, indicating different roles for the NLRP1 paralog genes in the context of STZ-induced T1D and suggesting that *Nlrp1a* may have an important role in the maintenance of the gut epithelial barrier. However, to our surprise, even after the administration of a cocktail of Abx to deplete the gut microbiota of NLRP1<sup>-/-</sup> mice, there was still an increase in Th17 cells in the PLNs, indicating that the driving mechanism is not the translocation of bacteria from the gut to the PLNs.

Recent studies have shown that innate immune receptors, such as TLR2, NOD2, and NLRP3 are expressed and functional in lymphocytes, thus, contributing to their differentiation into

distinct Th subtypes (Arbore et al., 2016; Bruchard et al., 2015; Reynolds et al., 2010). Therefore, we hypothesized that NLRP1 also specifically influences lymphoid-cell differentiation. Thus, we investigated the expression of *Nlrp1a* and *Nlrp1b* in both lymphoid and myeloid cells. Surprisingly, during the development of STZ-induced T1D, there was an increase in *Nlrp1b*, but not *Nlrp1a*, not only in lymphoid but also in myeloid cells, which is suggestive of a possible role of *Nlrp1b* in the activation of the inflammasome complex in myeloid cells, as well as in the differentiation of lymphocytes into distinct Th subtypes. However, even though there was a decrease in IL-1 $\beta$  in the absence of NLRP1, which is an important cytokine for the induction of Th17 cells, the increased susceptibility to STZ-induced T1D of NLRP1<sup>-/-</sup> mice was not observed in STZ-injected mice that lack important molecules for the assembly of the inflammasome complex, such as caspase-1/11, ASC, and IL-1R. These data suggest that the increase in Th17 cells in NLRP1-deficient mice does not rely on the inflammasome machinery. Subsequently, the role of NLRP1 specifically in T cells was analyzed, both *in vitro* and *in vivo*. Remarkably, in the absence of NLRP1, there was an increase in ROR $\gamma$ t expression and, consequently, in Th17 cells, suggesting that NLRP1 in T cells is a negative regulator of the Th17-cell-polarization program.

Lastly, through a genotype-guided assay, we demonstrated that the SNP rs12150220 A>T in *NLRP1* is significantly associated to reduced levels of Th17 cells and IL-17 in patients with T1D. This polymorphism has been previously associated to T1D in different populations (Magitta et al., 2009; Tang et al., 2013; Zurawek et al., 2010), although the exact mechanism still remains elusive. (Levandowski et al., 2013) demonstrated the effect of rs12150220 on IL-1 $\beta$  production in PBMCs. However, no other functional effects have yet been postulated for that variant. Intriguingly, both IL-17 and *NLRP1* genetics are involved in the pathogenesis of several autoimmune diseases, even though a cause-effect relationship has not been established. These results, in agreement with our experimental model of T1D, suggest that human NLRP1, similar to mouse *Nlrp1b*, is a negative regulator of Th17 cells.

In conclusion, our study demonstrates that NLRP1 acts as a negative regulator of Th17-cell-polarization programming, possibly through the expression of *Nlrp1b* in lymphoid cells; NLRP1 is also important for the integrity of the gut epithelial barrier, possibly through the expression of *Nlrp1a*. Both function synergistically to prevent the induction of Th17 cells in the early stages of STZ-induced T1D, thus, protecting from the development of the disease. Likewise, a genetically determined, increased constitutive NLRP1 activation in patients with T1D also correlates with decreased Th17 cell immune response, demonstrating that murine and human NLRP1 display similar features, making it a putative target for intervention during the early stages of the disease.

## STAR★METHODS

Detailed methods are provided in the online version of this paper and include the following:

### ● KEY RESOURCES TABLE

### ● RESOURCE AVAILABILITY

- Lead contact
- Materials availability
- Data and code availability

### ● EXPERIMENTAL MODEL AND SUBJECT DETAILS

- Mice
- Human blood samples and rs12150220 genotyping

### ● METHOD DETAILS

- Diabetes model
- FACS analysis of T cell subsets
- RT-PCR
- Western blot
- ELISA
- *In vitro* T cell differentiation
- Translocation and fecal transplantation assays

### ● QUANTIFICATION AND STATISTICAL ANALYSIS

## SUPPLEMENTAL INFORMATION

Supplemental information can be found online at <https://doi.org/10.1016/j.celrep.2021.109176>.

## ACKNOWLEDGMENTS

We are grateful to Franciele Pioto, MSc; Denise Ferraz; Cristiane Milanezi; and Wander Ribeiro for their technical assistance. The research leading to these results received funding from the São Paulo Research Foundation (FAPESP) under grant agreements 2013/08216-2 (Center for Research in Inflammatory Diseases [CRID]) 12/10395-02, 18/14815-0, and 16/10641, from FAEP (Fundação de Apoio ao Ensino, Pesquisa e Assistência do Hospital das Clínicas da Faculdade de Medicina de Ribeirão Preto) and CAPES (Coordenação de Aperfeiçoamento de Pessoal de Nível Superior).

## AUTHOR CONTRIBUTIONS

F.R.C.C designed and performed *in vitro* and *in vivo* experiments, analyzed the results, and wrote the manuscript. J.A.L., J.E.-O., and J.B.G. performed the *in vitro* assays and/or performed *in vivo* experiments; J.F.d.S., D.M.R., and M.C.F.-F. performed the western blot analysis and/or supported with the experiments involving human samples; N.O.S.C. and A.P. analyzed the SNP of NLRP1 and/or critically revised the manuscript; R.C.T. and J.S.S. edited the manuscript, provided scientific assistance, and critically revised the manuscript. D.C. provided intellectual support in addition to directing and supervising the study. All authors have read and agreed to the published version of the manuscript.

## DECLARATION OF INTERESTS

The authors declare no competing financial interests.

Received: April 8, 2020

Revised: November 30, 2020

Accepted: May 4, 2021

Published: May 25, 2021

## REFERENCES

- Arbore, G., West, E.E., Spolski, R., Robertson, A.A.B., Klos, A., Rheinheimer, C., Dutow, P., Woodruff, T.M., Yu, Z.X., O'Neill, L.A., et al. (2016). T helper 1 immunity requires complement-driven NLRP3 inflammasome activity in CD4<sup>+</sup> T cells. *Science* 352, aad1210.
- Arif, S., Moore, F., Marks, K., Bouckennooghe, T., Dayan, C.M., Planas, R., Vives-Pi, M., Powrie, J., Tree, T., Marchetti, P., et al. (2011). Peripheral and islet

interleukin-17 pathway activation characterizes human autoimmune diabetes and promotes cytokine-mediated  $\beta$ -cell death. *Diabetes* 60, 2112–2119.

Atkinson, M.A., Eisenbarth, G.S., and Michels, A.W. (2014). Type 1 diabetes. *Lancet* 383, 69–82.

Boyden, E.D., and Dietrich, W.F. (2006). Nalp1b controls mouse macrophage susceptibility to anthrax lethal toxin. *Nat. Genet.* 38, 240–244.

Bruchard, M., Reb  , C., Derang  re, V., Togb  , D., Ryffel, B., Boidot, R., Humblin, E., Hamman, A., Chalmin, F., Berger, H., et al. (2015). The receptor NLRP3 is a transcriptional regulator of Th2 differentiation. *Nat. Immunol.* 16, 859–870.

Carlos, D., Costa, F.R.C., Pereira, C.A., Rocha, F.A., Yaochite, J.N.U., Oliveira, G.G., Carneiro, F.S., Tostes, R.C., Ramos, S.G., Zamboni, D.S., et al. (2017). Mitochondrial DNA activates the NLRP3 inflammasome and predisposes to type 1 diabetes in murine model. *Front. Immunol.* 8, 164.

Chen, G.Y. (2014). Role of Nlrp6 and Nlrp12 in the maintenance of intestinal homeostasis. *Eur. J. Immunol.* 44, 321–327.

Chen, G., Shaw, M.H., Kim, Y.-G., and Nu  ez, G. (2009). NOD-like receptors: role in innate immunity and inflammatory disease. *Annu. Rev. Pathol.* 4, 365–398.

Costa, F.R.C., Fran  o, M.C.S., de Oliveira, G.G., Ignacio, A., Castoldi, A., Zamboni, D.S., Ramos, S.G., C  mara, N.O., de Zoete, M.R., Palm, N.W., et al. (2016). Gut microbiota translocation to the pancreatic lymph nodes triggers NOD2 activation and contributes to T1D onset. *J. Exp. Med.* 213, 1223–1239.

Devaraj, S., Tobias, P., Kasinath, B.S., Ramsamooj, R., Afify, A., and Jialal, I. (2011). Knockout of toll-like receptor-2 attenuates both the proinflammatory state of diabetes and incipient diabetic nephropathy. *Arterioscler. Thromb. Vasc. Biol.* 31, 1796–1804.

Elinav, E., Strowig, T., Kau, A.L., Henao-Mejia, J., Thaiss, C.A., Booth, C.J., Peaper, D.R., Bertin, J., Eisenbarth, S.C., Gordon, J.I., and Flavell, R.A. (2011). NLRP6 inflammasome regulates colonic microbial ecology and risk for colitis. *Cell* 145, 745–757.

Enam  lle, J.A., Davis, J., Merani, S., Toso, C., Elliott, J.F., Thiesen, A., and Shapiro, A.M. (2009). Inhibition of Th17 cells regulates autoimmune diabetes in NOD mice. *Diabetes* 58, 1302–1311.

Ferraro, A., Socci, C., Stabilini, A., Valle, A., Monti, P., Piemonti, L., Nano, R., Olek, S., Maffi, P., Scavini, M., et al. (2011). Expansion of Th17 cells and functional defects in T regulatory cells are key features of the pancreatic lymph nodes in patients with type 1 diabetes. *Diabetes* 60, 2903–2913.

Filippi, C.M., and von Herrath, M.G. (2008). Viral trigger for type 1 diabetes: pros and cons. *Diabetes* 57, 2863–2871.

Gon  alves, A.V., Margolis, S.R., Quirino, G.F.S., Mascarenhas, D.P.A., Rauch, I., Nichols, R.D., Ansaldo, E., Fontana, M.F., Vance, R.E., and Zamboni, D.S. (2019). Gasdermin-3 and caspase-7 are the key caspase-1/8 substrates downstream of the NAIP5/NLRC4 inflammasome required for restriction of *Legionella pneumophila*. *PLoS Pathog.* 15.

Haller, M.J., Schatz, D.A., Skyler, J.S., Krischer, J.P., Bundy, B.N., Miller, J.L., Atkinson, M.A., Becker, D.J., Baidal, D., DiMeglio, L.A., et al.; Type 1 Diabetes TrialNet ATG-GCSF Study Group (2018). Low-dose anti-thymocyte globulin (ATG) preserves  $\beta$ -cell function and improves HbA1c in new-onset type 1 diabetes. *Diabetes Care* 41, 1917–1925.

Herold, K.C., Vignali, D.A.A., Cooke, A., and Bluestone, J.A. (2013). Type 1 diabetes: translating mechanistic observations into effective clinical outcomes. *Nat. Rev. Immunol.* 13, 243–256.

Honkanen, J., Nieminen, J.K., Gao, R., Luopajarvi, K., Salo, H.M., Ilonen, J., Knip, M., Otonkoski, T., and Vaarala, O. (2010). IL-17 immunity in human type 1 diabetes. *J. Immunol.* 185, 1959–1967.

Hu, C., Ding, H., Li, Y., Pearson, J.A., Zhang, X., Flavell, R.A., Wong, F.S., and Wen, L. (2015). NLRP3 deficiency protects from type 1 diabetes through the regulation of chemotaxis into the pancreatic islets. *Proc. Natl. Acad. Sci. USA* 112, 11318–11323.

Joseph, J., Bittner, S., Kaiser, F.M.P., Wiendl, H., and Kissler, S. (2012). IL-17 silencing does not protect nonobese diabetic mice from autoimmune diabetes. *J. Immunol.* 188, 216–221.

Kim, H.S., Han, M.S., Chung, K.W., Kim, S., Kim, E., Kim, M.J., Jang, E., Lee, H.A., Youn, J., Akira, S., and Lee, M.S. (2007). Toll-like receptor 2 senses beta-cell death and contributes to the initiation of autoimmune diabetes. *Immunity* 27, 321–333.

Lee, G.R. (2018). The balance of th17 versus T<sub>reg</sub> cells in autoimmunity. *Int. J. Mol. Sci.* 19, 1–14.

Levandowski, C.B., Mailloux, C.M., Ferrara, T.M., Gowan, K., Ben, S., Jin, Y., McFann, K.K., Holland, P.J., Fain, P.R., Dinarello, C.A., and Spritz, R.A. (2013). NLRP1 haplotypes associated with vitiligo and autoimmunity increase interleukin-1 $\beta$  processing via the NLRP1 inflammasome. *Proc. Natl. Acad. Sci. USA* 110, 2952–2956.

Li, Y.Y., Pearson, J.A., Chao, C., Peng, J., Zhang, X., Zhou, Z., Liu, Y., Wong, F.S., and Wen, L. (2017). Nucleotide-binding oligomerization domain-containing protein 2 (Nod2) modulates T1DM susceptibility by gut microbiota. *J. Autoimmun.* 82, 85–95.

Magitta, N.F., B   Wolff, A.S., Johansson, S., Skinningsrud, B., Lie, B.A., Myhr, K.-M., Undlien, D.E., Joner, G., N  lsted, P.R., Kvien, T.K., et al. (2009). A coding polymorphism in NALP1 confers risk for autoimmune Addison's disease and type 1 diabetes. *Genes Immun.* 10, 120–124.

Marleau, A.M., Summers, K.L., and Singh, B. (2008). Differential contributions of APC subsets to T cell activation in nonobese diabetic mice. *J. Immunol.* 180, 5235–5249.

Masters, S.L., Gerlic, M., Metcalf, D., Preston, S., Pellegrini, M., O'Donnell, J.A., McArthur, K., Baldwin, T.M., Chevrier, S., Nowell, C.J., et al. (2012). NLRP1 inflammasome activation induces pyroptosis of hematopoietic progenitor cells. *Immunity* 37, 1009–1023.

Patterson, C.C., Dahlquist, G.G., Gy  r  s, E., Green, A., and Solt  sz, G.; EURODIAB Study Group (2009). Incidence trends for childhood type 1 diabetes in Europe during 1989–2003 and predicted new cases 2005–20: a multi-centre prospective registration study. *Lancet* 373, 2027–2033.

Rewers, M., and Ludvigsson, J. (2016). Environmental risk factors for type 1 diabetes. *Lancet* 387, 2340–2348.

Reynolds, J.M., Pappu, B.P., Peng, J., Martinez, G.J., Zhang, Y., Chung, Y., Ma, L., Yang, X.O., Nurieva, R.I., Tian, Q., and Dong, C. (2010). Toll-like receptor 2 signaling in CD4(+) T lymphocytes promotes T helper 17 responses and regulates the pathogenesis of autoimmune disease. *Immunity* 32, 692–702.

Shimada, K., Crother, T.R., Karlin, J., Dagvadorj, J., Chiba, N., Chen, S., Ramanujan, V.K., Wolf, A.J., Vergnes, L., Ojcius, D.M., et al. (2012). Oxidized mitochondrial DNA activates the NLRP3 inflammasome during apoptosis. *Immunity* 36, 401–414.

Soares, J.L.S., Fernandes, F.P., Patente, T.A., Monteiro, M.B., Parisi, M.C., Giannella-Neto, D., Corr  a-Giannella, M.L., and Pontillo, A. (2017). Gain-of-function variants in NLRP1 protect against the development of diabetic kidney disease: NLRP1 inflammasome role in metabolic stress sensing? *Clin. Immunol.* 187, 46–49.

Spanier, J.A., Sahli, N.L., Wilson, J.C., Martinov, T., Dileepan, T., Burrack, A.L., Finger, E.B., Blazar, B.R., Michels, A.W., Moran, A., et al. (2017). Increased effector memory insulin-specific CD4+ T cells correlate with insulin autoantibodies in patients with recent-onset type 1 diabetes 66, 3051–3060.

Sutterwala, F.S., Ogura, Y., Szczepanik, M., Lara-Tejero, M., Lichtenberger, G.S., Grant, E.P., Bertin, J., Coyle, A.J., Gal  n, J.E., Askenase, P.W., et al. (2006). Critical role for NALP3/CIAS1/cryopyrin in innate and adaptive immunity through its regulation of caspase-1. *Immunity* 24, 317–327.

Tang, L., Wang, L., Liao, Q., Wang, Q., Xu, L., Bu, S., Huang, Y., Zhang, C., Ye, H., Xu, X., et al. (2013). Genetic associations with diabetes: meta-analyses of 10 candidate polymorphisms. *PLoS ONE* 8, e70301.

Tye, H., Yu, C.H., Simms, L.A., de Zoete, M.R., Kim, M.L., Zakrzewski, M., Penington, J.S., Harapas, C.R., Souza-Fonseca-Guimaraes, F., Wockner, L.F., et al. (2018). NLRP1 restricts butyrate producing commensals to exacerbate inflammatory bowel disease. *Nat. Commun.* 9, 3728.

Uno, S., Imagawa, A., Okita, K., Sayama, K., Moriwaki, M., Iwahashi, H., Yamagata, K., Tamura, S., Matsuzawa, Y., Hanafusa, T., et al. (2007).

Macrophages and dendritic cells infiltrating islets with or without beta cells produce tumour necrosis factor- $\alpha$  in patients with recent-onset type 1 diabetes. *Diabetologia* 50, 596–601.

Vaarala, O. (2008). Leaking gut in type 1 diabetes. *Curr. Opin. Gastroenterol.* 24, 701–706.

Walker, L.S.K., and von Herrath, M. (2016). CD4 T cell differentiation in type 1 diabetes. *Clin. Exp. Immunol.* 1, 16–29.

Williams, T.M., Leeth, R.A., Rothschild, D.E., Coutermarsh-Ott, S.L., McDaniel, D.K., Simmons, A.E., Heid, B., Cecere, T.E., and Allen, I.C. (2015). The NLRP1 inflammasome attenuates colitis and colitis-associated tumorigenesis. *J. Immunol.* 194, 3369–3380.

Wlodarska, M., Thaïss, C.A., Nowarski, R., Henao-Mejia, J., Zhang, J.P., Brown, E.M., Frankel, G., Levy, M., Katz, M.N., Philbrick, W.M., et al. (2014).

NLRP6 inflammasome orchestrates the colonic host-microbial interface by regulating goblet cell mucus secretion. *Cell* 156, 1045–1059.

Yang, X.O., Panopoulos, A.D., Nurieva, R., Chang, S.H., Wang, D., Watowich, S.S., and Dong, C. (2007). STAT3 regulates cytokine-mediated generation of inflammatory helper T cells. *J. Biol. Chem.* 282, 9358–9363.

Yaochite, J.N., Calari-Oliveira, C., Davanzo, M.R., Carlos, D., Malmegrim, K.C., Cardoso, C.R., Ramalho, L.N., Palma, P.V., da Silva, J.S., Cunha, F.Q., et al. (2013). Dynamic changes of the Th17/Tc17 and regulatory T cell populations interfere in the experimental autoimmune diabetes pathogenesis. *Immunobiology* 218, 338–352.

Zurawek, M., Fichna, M., Januszkiewicz-Lewandowska, D., Gryczyńska, M., Fichna, P., and Nowak, J. (2010). A coding variant in NLRP1 is associated with autoimmune Addison's disease. *Hum. Immunol.* 71, 530–534.



## STAR★METHODS

### KEY RESOURCES TABLE

REAGENT or RESOURCE	SOURCE	IDENTIFIER
<b>Antibodies</b>		
Rat anti-mouse IL-17A – PE (clone TC11-18H10)	BD Biosciences	Cat #559502; RRID:AB_397256
Rat anti-mouse IL-17A – V450 (clone TC11-18H10)	BD Biosciences	Cat #560522; RRID:AB_1727540
Mouse anti-human IL-17A – BV421 (clone N49-653)	BD Biosciences	Cat #562933; RRID:AB_2737902
Rat anti-mouse Foxp3 – PE (clone MF23)	BD Biosciences	Cat #560408; RRID:AB_1645251
Rat anti-mouse IFN $\gamma$ – PE-Cy7 (clone XMG1.2)	BD Biosciences	Cat #557649; RRID:AB_396766
Rat anti-mouse IFN $\gamma$ – APC (clone XMG1.2)	BD Biosciences	Cat #554413; RRID:AB_398551
Mouse anti-human IFN $\gamma$ – BV605 (clone B27)	BD Biosciences	Cat #562974; RRID:AB_2737926
Rat anti-mouse CD4 – PerCP-Cy 5.5 (clone RM4-5)	BD Biosciences	Cat #550954; RRID:AB_393977
Mouse anti-human CD4 – FITC (clone RPA-T4)		Cat #555346; RRID:AB_395751
Hamster anti-mouse CD3e – APC (clone 145-2C11)	BD Biosciences	Cat #553066; RRID:AB_398529
Hamster anti-mouse CD3e – FITC (clone 145-2C11)	BD Biosciences	Cat #553062; RRID:AB_394595
Hamster anti-mouse CD3e – APC-Cy7 (clone 145-2C11)	BD Biosciences	Cat #557596; RRID:AB_396759
Mouse anti-human CD3 – PE-Cy7 (clone UCHT1)	BD Biosciences	Cat #563423; RRID:AB_2738196
Rat anti-mouse CD8a – FITC (clone 53-6.7)	BD Biosciences	Cat #553031; RRID:AB_394569
Rat anti-mouse CD8a – BV605 (clone 53-6.7)	BD Biosciences	Cat #563152; RRID:AB_2738030
Mouse anti-human CD8 – APC-Cy7 (clone SK1)	BD Biosciences	Cat #557834; RRID:AB_396892
Rat anti-mouse CD11b – APC-Cy7 (clone M1/70)	BD Biosciences	Cat #557657; RRID:AB_396772
Hamster anti-mouse CD11c – PE-Cy7 (clone HL3)	BD Biosciences	Cat #558079; RRID:AB_647251
Mouse anti-human CD45RO – PE (clone UCHL1)	BD Biosciences	Cat #555493; RRID:AB_395884
Mouse anti-human CD45RA – APC (clone HI100)	BD Biosciences	Cat #561884; RRID:AB_10893597
Rat anti-mouse IL-6 – PE (clone MP5-20F3)	BD Biosciences	Cat #554401; RRID:AB_395367
Rat anti-mouse IL-12 – APC (clone C15.6)	BD Biosciences	Cat #554480; RRID:AB_398560
Mouse anti-Stat3 (Py705) – PE-CF594 (clone 4/P-STAT3)	BD Biosciences	Cat #562673; RRID:AB_2737714
Rat anti-mouse CD19 – FITC (clone 1D3)	BD Biosciences	Cat #557398; RRID:AB_396681
<b>Chemicals, peptides, and recombinant proteins</b>		
Gentamicin	GIBCO	Cat #15750-060
Ionomycin	Sigma-Aldrich	Cat #I0634
Vancomycin	Sigma-Aldrich	Cat #V1130
Ampicillin	Sigma-Aldrich	Cat #A0166
Neomycin	Sigma-Aldrich	Cat #N1876
Metronidazole	Sigma-Aldrich	Cat #M1547
Streptozocin	Sigma-Aldrich	Cat #S0130
Phorbol 12-myristate 13-acetate	Sigma-Aldrich	Cat #P8139
Ficoll-Paque Plus	GE Healthcare Life Sciences	Cat #17-1440-02
Recombinant mouse IL-6	R&D Systems	Cat #406-ML
Recombinant mouse IL-23	R&D Systems	Cat #1887-ML
Recombinant mouse IL-1 $\beta$ /IL-1F2	R&D Systems	Cat #401-ML
TGF-beta 1 recombinant protein	GIBCO	Cat #PHG9202
Purified NA/LE Hamster anti-mouse CD3e (clone 145-2C11)	BD Biosciences	Cat #553057

(Continued on next page)

**Continued**

REAGENT or RESOURCE	SOURCE	IDENTIFIER
Purified NA/LE Hamster anti-mouse CD28 (clone 37.51)	BD Biosciences	Cat #553294
Anti-NLRP1 antibody	Abcam	Cat #ab3683
Goat anti-rabbit IgG H&L (HRP)	Abcam	Cat #ab6721
$\beta$ -actin antibody	Cell Signaling	Cat #4967
Tris base	BioRad	Cat #1610719
Nonidet P40	Roche	Cat #11754599001
PMSF (Phenylmethanesulfonyl fluoride)	Sigma-Aldrich	Cat #P7626

**Critical commercial assays**

CD4 <sup>+</sup> T cell isolation kit, mouse - MACS	Miltenyi Biotec	Cat #130-104-454
LS Columns - MACS	Miltenyi Biotec	Cat #130-042-401
QuadroMACS separator	Miltenyi Biotec	Cat #130-090-976
GolgiStop Protein Transport Inhibitor	BD Biosciences	Cat #554724
Phosflow Lyse/Fix Buffer I	BD Biosciences	Cat #558049
Phosflow Perm/Wash Buffer I	BD Biosciences	Cat #557885
SV Total RNA isolation system	Promega	Cat #Z3105
DNeasy Blood & Tissue kits	QIAGEN	Cat #69504
TaqMan SNP Genotyping Assay, human	Applied Biosystems	Cat #4351374
TaqMan Genotyping Master Mix	Applied Biosystems	Cat #4371353
Bradford reagent	Supelco	Cat #B6916
Luminata Forte HRP Substrate	Millipore	Cat #ELLUF0100
SIGMAFAST Protease Inhibitor Tablets	Sigma-Aldrich	Cat #S8820
Mouse IFN-gamma DuoSet ELISA	R&D Systems	Cat #DY485
Mouse IL-1 beta/IL-1F2 DuoSet ELISA	R&D Systems	Cat #DY401
Mouse IL-1 alpha/IL-1F1 DuoSet ELISA	R&D Systems	Cat #DY400
Mouse IL-17 DuoSet ELISA	R&D Systems	Cat #DY421
Mouse IL-18 DuoSet ELISA	R&D Systems	Cat #DY7625-05
Human IL-17 DuoSet ELISA	R&D Systems	Cat #DY317
Human IFN-gamma DuoSet ELISA	R&D Systems	Cat #DY285

**Experimental models: Organisms/strains**

Mouse: C57BL/6	The Jackson Laboratory	JAX: 000664
Mouse: B6.129S6- <i>Nlrp1b</i> <sup>tm1Bhk</sup> /J	The Jackson Laboratory	JAX: 021301
Mouse: B6.129S7- <i>Rag1</i> <sup>tm1Mom</sup> /J	The Jackson Laboratory	JAX: 002216
Mouse: ASC <sup>-/-</sup>	<a href="#">Sutterwala et al., 2006</a>	N/A
Mouse: B6.129(Cg)- <i>Il1r1</i> <sup>tm1.1Rbl</sup> /J	The Jackson Laboratory	JAX: 028398
Mouse: Caspase1 <sup>-/-</sup>	<a href="#">Gonçalves et al., 2019</a>	N/A
Mouse: NOD/ShiLtJ	The Jackson Laboratory	JAX: 001976

**Oligonucleotides**

Primers for RT-PCR, see <a href="#">Table S2</a>	N/A	N/A
--	-----	-----

**Software and algorithms**

FlowJo analysis software	BD Biosciences	<a href="https://www.flowjo.com/solutions/flowjo/downloads">https://www.flowjo.com/solutions/flowjo/downloads</a>
Diva	BD Biosciences	N/A
ImageQuant 1.3 software	GE Healthcare	N/A
GraphPad Prism 6.07	GraphPad	<a href="https://www.graphpad.com/">https://www.graphpad.com/</a>

**Other**

Accu-Chek Performa Nano	Roche	Cat # 4015630981854
FACSCanto II Cell Analyzer	BD Biosciences	Cat #338962

(Continued on next page)

### Continued

REAGENT or RESOURCE	SOURCE	IDENTIFIER
FACSria III Cell Sorter	BD Biosciences	Cat #648282
Nanodrop 2000	Thermo Fisher Scientific	Cat # ND-2000
StepOnePlus Real-Time PCR System	Applied Biosystems	Cat #4376600
Sub-Cell GT Horizontal Electrophoresis cell (Power Pac HC)	BioRad	Cat #1645050
Mini Trans-Blot Cell	BioRad	Cat #1703930

## RESOURCE AVAILABILITY

### Lead contact

Further information and requests for resources and reagents should be directed to and will be fulfilled by the lead contact, Daniela Carlos ([danicar@usp.br](mailto:danicar@usp.br)).

### Materials availability

This study did not generate new unique reagents.

### Data and code availability

This study did not generate or analyze datasets or code.

## EXPERIMENTAL MODEL AND SUBJECT DETAILS

### Mice

8-10 weeks-old male C57BL/6 wild-type (WT) mice and mice deficient in NLRP1, ASC, IL-1R and caspase-1 were used. NOD/LtJ mice were obtained from The Jackson Laboratory. Mice were housed and bred under specific pathogen-free conditions. All animal procedures were approved by our local ethics committee (Comit  de  tica no Uso de Animais – CEUA – from Ribeir o Preto Medical School, University of Sao Paulo; Process number 139/2012).

### Human blood samples and rs12150220 genotyping

Briefly, 40 mL of blood were collected from T1D patients (Table S1), diluted in PBS (1:1) and mixed with Fycoll-Hypaque (also in a 1:1 proportion). Then, the blood was centrifuged at 2000 rpm for 30 min at 25 C and the PBMC were collected. These cells were washed twice in PBS and suspended in X-VIVO<sup>TM</sup> (Lonza) culture media. For the genotyping assays (human *Nlrp1* polymorphism, rs12150220), DNA was extracted from PBMC using a DNeasy Blood & Tissue kit  (QIAGEN) and the analysis was performed with a Taqman SNP Genotyping Assay (Applied Biosystems), following the manufacturer’s recommendations. All experiments with human samples were performed in accordance with the ethical standards established by the Declaration of Helsinki and with our local Ethics Committee in Research (Comit  de  tica em Pesquisa da Faculdade de Medicina de Ribeir o Preto – Universidade de S o Paulo, protocol number 1.887.263).

## METHOD DETAILS

### Diabetes model

Male C57BL/6, ranging from 8 to 10 weeks of age, were injected for five consecutive days, intraperitoneally (i.p.), with 40 mg/kg STZ (Sigma-Aldrich). STZ was diluted in sodium citrate buffer (pH = 4.5), and immediately injected after preparation. Blood samples were collected from the tail vein of non-fasted mice and glycemia was analyzed with the glucometer system AccuCheck Nano (Accu-Check ). Mice were considered diabetic after two consecutive readings above 200 mg/dL. Control mice received only sodium citrate buffer (vehicle) i.p. for five consecutive days.

### FACS analysis of T cell subsets

Phenotypical analysis of cells isolated from either PLNs or PBMC were performed through flow cytometry. For the detection of Treg, Th17/Tc17 and Th1/Tc1 cells, the expression of Foxp3, IL-17 and IFN-  within CD3 CD4  and CD3 CD8  T cells or within CD45RA CD45RO CD3 CD4  memory T cells was determined after *in vitro* stimulation with 50 ng/ml phorbol myristate acetate (PMA – Sigma Aldrich), 500 ng/ml ionomycin (Sigma Aldrich) and, subsequently, Golgi Stop (1,000X; BD). Cells were then fixed in 4% paraformaldehyde diluted in PBS and permeabilized in PBS containing 1% fetal bovine serum (FBS), 0.2% saponin and 0.1% sodium azide. Monoclonal antibodies were added, and cells were incubated for 20 min at 4 C. After the staining, the cells were

washed and fixed in 1% paraformaldehyde diluted in phosphate buffer saline (PBS) and further analyzed in a FACSCanto II. We also analyzed the presence of IL-6<sup>+</sup> or IL-12<sup>+</sup> CD11b<sup>+</sup>CD11c<sup>+</sup> dendritic cells. Alternatively, CD4<sup>+</sup> T cells were purified from cells of the spleen and lymph nodes of WT and NLRP1<sup>-/-</sup> mice (CD4 T Cell Isolation Kit – Milteny Biotec) and were stimulated with rIL-6 (20ng/mL – R&D Systems) for 30min. Then, cells were collected and analyzed for pSTAT3 (pY705) with the PhosFlow kit (BD Biosciences).

### RT-PCR

RNA samples from PLNs or PBMC were obtained with an RNA extraction Kit (Promega) and quantified using a NanoDrop 2000® equipment (Thermo Fisher Scientific). For the analysis of the relative expression of *Nlrp1a*, *Nlrp1b*, *Ifnγ*, *Rorc*, *Rora*, *Stat3*, *Il1r1*, *Il23r*, *Il17a*, *Il22* and *Nlrp1* (human), RNA samples were analyzed using SYBR Green in a Step One Plus® system (Applied Biosystems). Primers sequences for specific genes are provided in [Table S2](#).

### Western blot

Isolated CD4<sup>+</sup> T cells from WT mice were polarized into Th17 cells. Then, total protein extraction was performed in lysis buffer [50 mmol/L Tris-HCl (pH 7.4) containing 1% Nonidet P-40, 0.5% sodium deoxycholate, 150 mmol/L NaCl, 1 mmol/L EDTA, 0.1% sodium dodecyl sulfate (SDS), 1 mmol/L phenylmethylsulfonyl fluoride (PMSF), 1 μg/mL pepstatin A, 1 μg/mL leupeptin and 1 μg/mL aprotinin]. Protein concentration was assessed by the Bradford method (Bradford Reagent, Sigma, cat. B6916). Then, 20 μg of protein was separated by electrophoresis on 8% SDS polyacrylamide gel and transferred to a nitrocellulose membrane for western blotting. Membranes were blocked with Tris-buffered solution (TBS) containing 3% albumin overnight at 4°C. Membranes were then incubated with primary antibody overnight at 4°C. Then, membranes were washed 3x with TBS-Tween 20 and incubated with a specific secondary antibody. Immunocomplexes were detected by chemiluminescence reaction (Luminata Forte HRP Substrate; Millipore, USA), and densitometric analysis was performed with ImageQuant 1.3 software. Protein expression levels were normalized to the internal housekeeping protein (β-actin). The primary and second antibodies used in this set of experiments were anti-NLRP1 (dilution 1:1000, Abcam, ab3683), anti-β-actin (dilution 1:3000, Cell Signaling, # 4967) and anti-rabbit IgG (dilution 1:5000, Abcam, ab6721).

### ELISA

The production of cytokines (IFN-γ, IL-1β, IL-1α, IL-17 and IL-18) in the pancreatic tissue of mice, and IL-17 and IFN-γ in the serum of T1D patients was quantified by ELISA using specific kits and following the instructions from the manufacturer (all kits were purchased from R&D).

### In vitro T cell differentiation

CD4<sup>+</sup> T cells were purified from spleen and lymph nodes (LNs) with anti-CD4 microbeads (Milteny Biotec) and then further sorted as naive CD4<sup>+</sup>CD44<sup>lo</sup>CD62L<sup>hi</sup> T cells using a FACS Aria III sorter (BD Biosciences). Sorted cells were activated with plate-bound anti-CD3 (4 μg/mL) and soluble anti-CD28 (2 μg/mL, both from BD Biosciences) in the presence of polarizing cytokines. For Th17 differentiation, the following reagents were used: 20 ng/mL of IL-6, 50 ng/mL of IL-23 and 20 ng/mL of IL-1β (R&D Systems). Cells were cultured for 3 days and then analyzed by flow cytometry for IL-17 production or by RT-PCR for the expression of molecules involved in Th17 cell differentiation.

### Translocation and fecal transplantation assays

Mice were given daily doses vancomycin (0.96 mg), ampicillin (1.86 mg), neomycin sulfate (1.86 mg) and metronidazole (1.86 mg) diluted in 300 μL of drinking water by gavage for 2 weeks before the injections with STZ. All antibiotics (Abx) were purchased from Sigma-Aldrich. For fecal transplantation, mice were administered with the daily doses of Abx for 3 weeks, and then received by gavage 200 μL of fecal samples from C57BL/6 WT mice diluted in PBS. Ten days later, these NLRP1<sup>-/-</sup> (designated as NLRP1<sup>-/-</sup>[WT]) mice were injected with 5 doses of STZ and were analyzed for blood glucose levels 10 days later.

### QUANTIFICATION AND STATISTICAL ANALYSIS

All analyses were performed using Graphpad Prism (version 6.0). Normal distribution and homogeneity of variance were tested in all variables. For normal distribution and homogeneous variance, parametric tests were used. When the variance was statistically different, unpaired t test with Welch's correction was performed. The results were expressed as standard ± standard error of the mean (SEM). Observed differences were considered statistically significant when  $p < 0.05$ .